Amirkabir Journal of Mechanical Engineering

Amirkabir J. Mech. Eng., 53(4) (2021) 491-494
DOI: 10.22060/mej.2020.17759.6661

Kinematic and dynamic performance evaluation of a four degrees of freedom parallel robot

P. Ghaf-Ghanbari, M. Taghizadeh* , M. Mazare

School of Mechanical Engineering, Shahid Beheshti University, Tehran, Iran

ABSTRACT: In this paper, the performance four-degree-of-freedom parallel manipulator with Schönflies motion is evaluated from kinematic and dynamic points of view. Its low inertia makes it a suitable choice for pick-and-place applications, which demand high velocity and acceleration. So, the dynamic characteristics of the robot are of high importance. Moreover, parallel robots suffer from a small workspace, on which their singularities put additional constrain. Hence, this paper studies the kinematic and dynamic behavior of the robot in-depth to give a clear perspective to path planning and its applications. To perform kinematic analysis, constraint equations are derived based on the geometric method, and then Jacobian matrices are determined via velocity analysis. By considering the constraint equations and joint limits, reachable workspace is determined, applying point-to-point search algorithm and singularities are identified by the inverse and direct Jacobian matrices. For dynamic modeling, Euler-Lagrange formulation is applied and both kinematic and dynamic models are verified by the results obtained from mechanism simulation in ADAMS software. Furthermore, for evaluation of the robot performance, pressure angles are employed to show the equality of motion/force transmission, and dynamic indices based on joint space inertia matrix are applied to illustrate its dynamic behavior.

Review History:

Received: Jan. 19, 2020
Revised: Mar. 14, 2020-03-14
Accepted: May, 03, 2020
Available Online: May, 16, 2020

Keywords:

four-degree-of-freedom parallel robot
Schönflies motion
Kinematics
Dynamics
Performance Evaluation

1- Introduction

Parallel Kinematic Manipulators (PKM) are closed-loop kinematic chain mechanisms comprising of several independent serial chins, connecting the end-effector to the base. This constrained structure gives them capabilities like high accuracy, velocity, stiffness, payload capacity, and great dynamic performance, and makes them an excellent choice for Pick-and-place (PnP) applications. Thanks to their light-weight and low-inertia structure, delta type Schönflies motion (3T1R) PKMs are extensively employed for PnP applications. Aside from all positive points, PKMs suffer from some drawbacks such as small workspace and singular configurations. These limitations together with the demanding tasks for which they are planned have been the motivation behind numerous researches on performance evaluation criteria [1-4].

2- Methodology

The PKM under study is a modification on the redundantly actuated Veloce [5], which is composed of four identical R-(SS)2 arms, connecting the base to the end-effector. As shown in Fig. 1, by shifting the connection of two opposite arms to the end-effector along with opposite directions and adding a couple of revolute joints, the mechanism will be able to generate Schönflies motion, with rotation around the horizontal axis [6].

The structure of one arm of the manipulator is illustrated in Fig. 2. The loop-closure equation for the ith arm is written as

$$\mathbf{r}_P + \varepsilon_i l_4 \hat{\boldsymbol{w}}_i = l_1 \hat{\boldsymbol{e}}_i + l_2 \hat{\boldsymbol{u}}_i + l_3 \hat{\boldsymbol{v}}_i \tag{1}$$

$$\varepsilon_i = \begin{cases} \sec\beta_i & i=1,4 \\ -\sec\beta_i & i=2,3 \end{cases} \tag{2}$$

where, $\mathbf{r}_P = \begin{bmatrix} x_P & y_P & z_P \end{bmatrix}^T$.

Squaring both sides of Eq. (1) and simplifying the result yields the inverse kinematic equation as

$$\begin{gathered} \theta_i = 2\arctan\left(\frac{-C_{i1} \pm \sqrt{C_{i1}^2 - \left(C_{i3}^2 - C_{i2}^2\right)}}{C_{i3} - C_{i2}} \right) \\ C_{i1} = 2l_2 \left(\mathbf{r}_P + \varepsilon_i l_4 \hat{\boldsymbol{w}}_i - \mathbf{r}_{Ai}\right) \cdot \hat{\xi}_3 \\ C_{i2} = -2l_2 \left(\mathbf{r}_P + \varepsilon_i l_4 \hat{\boldsymbol{w}}_i - \mathbf{r}_{Ai}\right) \cdot \left\{\hat{\xi}_1 c\alpha_i + \hat{\xi}_2 s\alpha_i\right\} \\ C_{i3} = \left(\mathbf{r}_P + \varepsilon_i l_4 \hat{\boldsymbol{w}}_i - \mathbf{r}_{Ai}\right)^2 + l_2^2 - l_3^2 \\ \hat{\xi}_1 = [1 \quad 0 \quad 0]^T,\ \hat{\xi}_2 = [0 \quad 1 \quad 0]^T,\ \hat{\xi}_3 = [0 \quad 0 \quad 1]^T \end{gathered} \tag{3}$$

*Corresponding author's email: mo_taghizadeh@sbu.ac.ir

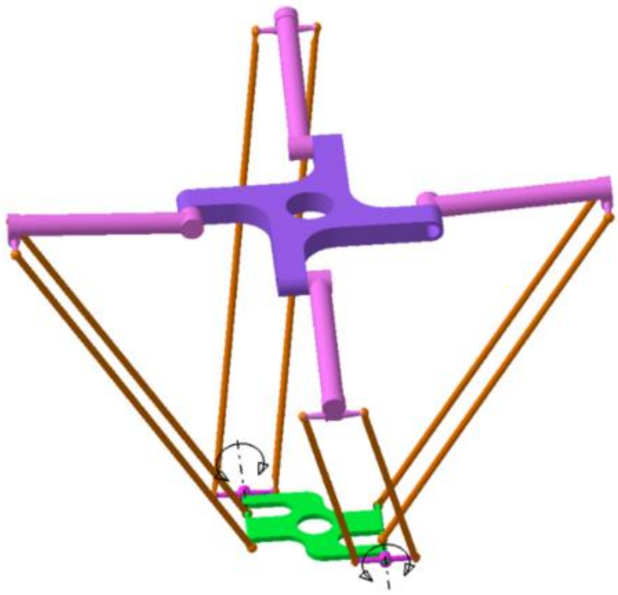

Fig. 1. CAD model of the Schönflies PKM

For velocity analysis, Eq. (1) is differentiated with respect to time, which gives the Jacobian matrix, mapping the joints' velocity to the velocity of the end-effector.

$$J_\theta \dot{\boldsymbol{\Theta}} = J_X \dot{\boldsymbol{\mathcal{X}}}$$

$$J_{\theta i}=l_2(\hat{\boldsymbol{n}}_i \times \hat{\boldsymbol{u}}_i).\hat{\boldsymbol{v}}_i\,, \qquad J_\theta=\mathrm{diag}[J_{\theta 1}\quad J_{\theta 2}\quad J_{\theta 3}\quad J_{\theta 4}]$$
$$J_{Xi}=\begin{bmatrix}\hat{\boldsymbol{v}}_i^T & \left(\hat{\xi}_2\times \mathbf{r}^O_{PCi}\right).\hat{\boldsymbol{v}}_i\end{bmatrix},\quad J_X=\begin{bmatrix}J_{X1}^T & J_{X2}^T & J_{X3}^T & J_{X4}^T\end{bmatrix}^T \tag{4}$$

Applying Euler-Lagrange formulation, the dynamic model is obtained as,

$$\boldsymbol{\tau}=\boldsymbol{\mathcal{M}}\ddot{\boldsymbol{\mathcal{X}}}+\boldsymbol{\mathcal{C}}\dot{\boldsymbol{\mathcal{X}}}+\boldsymbol{\mathcal{G}}+\boldsymbol{\mathcal{F}}$$
$$\boldsymbol{\mathcal{M}}=\boldsymbol{M}_a\boldsymbol{J}+\boldsymbol{J}^{-T}\boldsymbol{M}_P\quad,\quad \boldsymbol{\mathcal{C}}=\boldsymbol{M}_a\dot{\boldsymbol{J}} \tag{5}$$
$$\boldsymbol{\mathcal{G}}=\boldsymbol{G}_a+\boldsymbol{J}^{-T}\boldsymbol{G}_P\quad,\quad \boldsymbol{\mathcal{F}}=-\boldsymbol{J}^{-T}\boldsymbol{F}$$

where,

$$\boldsymbol{M}_a=\frac{1}{6}l_2^2(2m_U+3m_L)\boldsymbol{I}_{4\times4}\,,\qquad \boldsymbol{G}_a=-\frac{1}{2}l_2(m_U+m_L)\mathrm{g}\cos\boldsymbol{\Theta}$$

$$\boldsymbol{M}_P=\begin{bmatrix}(m_e+2m_L)\boldsymbol{I}_{3\times3} & \boldsymbol{0}_{3\times1}\\ \boldsymbol{0}_{1\times3} & I^P_{P_{yy}}+2m_Ll_4^2\end{bmatrix}$$

$$\boldsymbol{G}_P=-(m_e+2m_L)\begin{bmatrix}\mathbf{g}^T & 0\end{bmatrix}^T,\qquad \boldsymbol{J}=\boldsymbol{J}_\theta^{-1}\boldsymbol{J}_X$$

3- Performance Evaluation

To describe the motion/force transmission ability of a parallel mechanism, two distinct pressure angles are defined.

$$\mu_i=\cos^{-1}\hat{\boldsymbol{v}}_i^T\left(\hat{\boldsymbol{n}}_i\times\hat{\boldsymbol{u}}_i\right) \tag{6}$$

$$\vartheta=\cos^{-1}\frac{\left(\hat{\boldsymbol{v}}_{14}\times\hat{\boldsymbol{v}}_{23}\right)^T\hat{\mathbf{s}}}{\hat{\boldsymbol{v}}_{14}\times\hat{\boldsymbol{v}}_{23}} \tag{7}$$

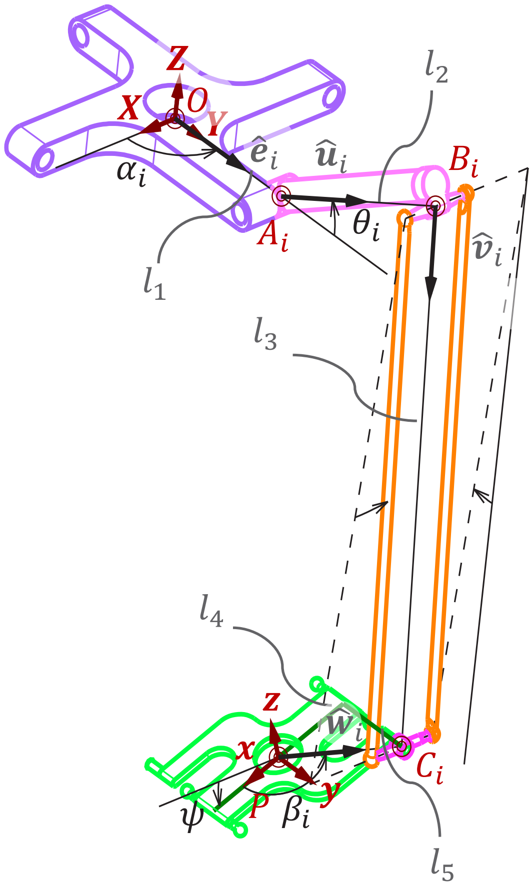

Fig. 2. Coordinate frames and variables of the arm

where μ_i shows the motion/force transmitted from the active joint of the i-th arm to the end-effector, and ϑ indicates the force transmitted from the end-effector to the passive joints of the other arms when their active joints are locked. The local transmission index for kinematic evaluation of the mechanism is defined as,

$$\mathrm{LTI}=\min\left\{\left|\cos\mu_i\right|,\left|\cos\vartheta\right|\right\} \tag{8}$$

PnP applications require high acceleration devices, and this makes the inertia forces of the robot a decisive factor. Thus, the mean value of the principal elements of the joint space inertia matrix is defined as Joint-Reflected Inertia (JIR) and represents the overall inertial level of the parallel manipulator for inertia matching [7]. The Coefficient of Variation of joint-space Inertia (CVI) index is another dynamic index, showing the imbalance of inertia property among arms, and is defined [8],

$$\mathrm{CVI}=\frac{1}{I_{\mathrm{ave}}}\sqrt{\frac{1}{n}\sum_{i=1}^{n}\left(I_{ii}-I_{\mathrm{ave}}\right)^2} \tag{9}$$

4- Simulation Results

Three performance indices for a section cut crossing the workspace at z=-700 mm are shown in Figs. 3 to 5. As depicted in Fig. 3, the PKM demonstrates poor performance when ψ=0°, however as this angle increases to -45°, this index increases to

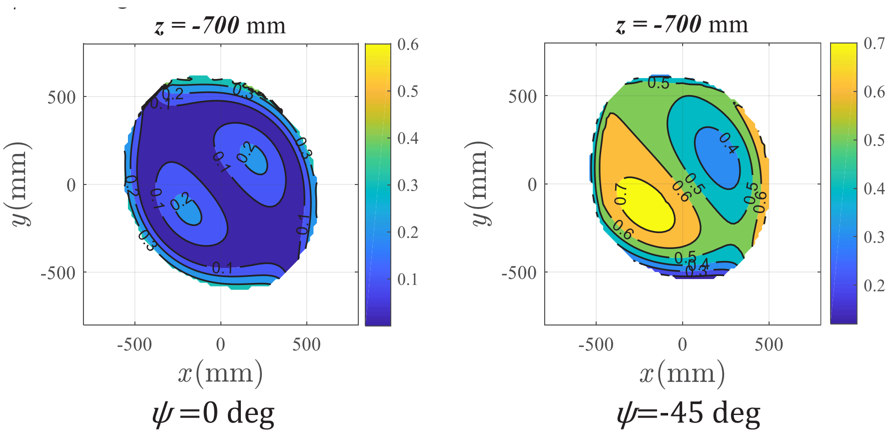

Fig. 3. LTI at *z*=-700 mm

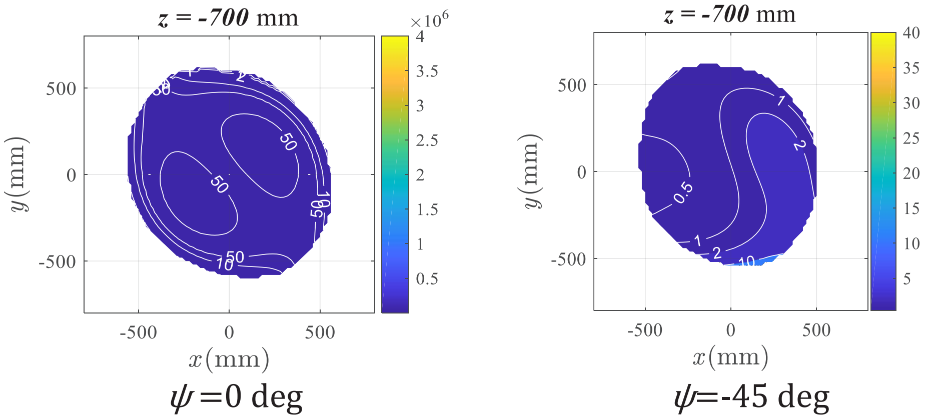

Fig. 4. JRI at *z*=-700 mm

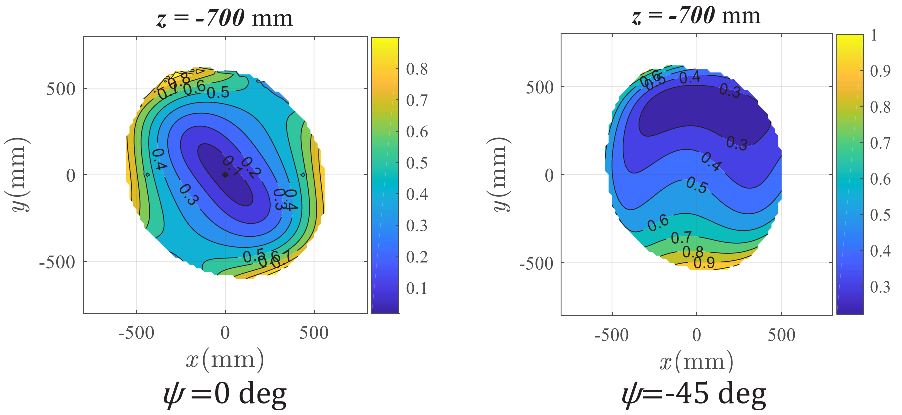

Fig. 5. CVI at *z*=-700 mm

higher values. JRI distribution illustrated in Fig. 4 reveals that when ψ =-45° this index is less than 10 for central area, while for horizontal configuration this index increases considerably.

According to Fig. 5, for ψ =-45° the distribution of CVI over the section is more uniform. For ψ =0° the central area offers better performance.

5- Conclusion

This paper addressed the performance evaluation of a Schönflies robot. It was shown that this robot demonstrates poor performance in the horizontal configuration of the end-effector, while for other configurations, the performance improves.

References

[1] P. C. Lee, J. J. Lee, On the kinematics of a new parallel mechanism with Schoenflies motion, Robotica, 34(9) (2016) 2056–2070.

[2] M. Mazare, M. Taghizadeh, m. R. Najafi, Kinematic analysis and design of a novel 3-DOF translational parallel robot, International Journal of Automation and Computing, 14(4) (2016) 432–441.

[3] S. Liu, T. Huang, J. Mei, X. Zhao, P. Wang, Optimal Design of a 4-DOF SCARA Type Parallel Robot Using Dynamic Performance Indices and Angular Constraints, ASME Journal of Mechanisms and Robotics, 4(3)(2012) 031005-031005-10.

[4] H. Shao, L. Wang, L. Guan, J. Wu, Dynamic manipulability and optimization of a redundant three DOF planar parallel manipulator, in: 2009 ASME/IFToMM International Conference on Reconfigurable Mechanisms and Robots, London, 2009.

[5] “Penta Veloce,” [Online]. Available: https://pentarobotics.com/products/#brochure.

[6] G. Wu, Kinematic Analysis and Optimal Design of a Wall-mounted Four-limb Parallel Schönflies-motion Robot for Pick-and-place Operations, Journal of Intelligent and Robotic Systems, 85(3-4) (2016) 663–677.

[7] Z. F. Shao, X. Tang, X. Chen, L. P. Wang, Research on the inertia matching of the Stewart parallel manipulator, Robotics and Computer-Integrated Manufacturing, 28 (2012) 649–659.

[8] J. Mo, Z. F. Shao, L. Guan, F. Xie, X. Tang, Dynamic performance analysis of the X4 high-speed pick-and-place parallel robot, Robotics and Computer–Integrated Manufacturing, 46(2017) 48-57.

HOW TO CITE THIS ARTICLE

P. Ghaf-Ghanbari, M. Taghizadeh, M. Mazare, Kinematic and dynamic performance evaluation of a four degrees of freedom parallel robot, Amirkabir J. Mech. Eng., 53(4) (2021) 491-494

DOI: 10.22060/mej.2020.17759.6661